The mechanisms underlying the effects of AMH on Mullerian duct regression in male mice

Yamamoto, Anzu ; Omotehara, Takuya ; Miura, Yuuka ; Takada, Tadashi ; Yoneda, Naoki ; Hirano, Tetsushi ; Mantani, Youhei ; Kitagawa, Hiroshi…

(Citation)
Journal of Veterinary Medical Science,80(4):557-567

(Issue Date)
2018-04

(Resource Type)
journal article

(Version)
Version of Record

(URL)
https://hdl.handle.net/20.500.14094/90004886

The Journal of Veterinary Medical Science

FULL PAPER

Anatomy

The mechanisms underlying the effects of AMH on Müllerian duct regression in male mice

Anzu YAMAMOTO[1)], Takuya OMOTEHARA[3)], Yuuka MIURA[1)], Tadashi TAKADA[1)], Naoki YONEDA[1)], Tetsushi HIRANO[4)], Youhei MANTANI[2)], Hiroshi KITAGAWA[2)], Toshifumi YOKOYAMA[1)] and Nobuhiko HOSHI[1)]*

[1)]Laboratory of Animal Molecular Morphology, Department of Animal Science, Graduate School of Agricultural Science, Kobe University, 1-1 Rokkodai, Nada, Kobe, Hyogo 657-8501, Japan
[2)]Laboratory of Histophysiology, Department of Animal Science, Graduate School of Agricultural Science, Kobe University, 1-1 Rokkodai, Nada, Kobe, Hyogo 657-8501, Japan
[3)]Department of Anatomy, Tokyo Medical University, 6-1-1 Shinjuku, Shinjuku, Tokyo 160-8402, Japan
[4)]Division of Drug and Structural Research, Life Science Research Center, University of Toyama, 2630 Sugitani, Toyama 930-0194, Japan

ABSTRACT. Anti-Müllerian hormone (AMH) produced in the developing testis induces the regression of the Müllerian duct, which develops into the oviducts, uterus and upper vagina. In our true hermaphrodite mouse with an ovary on one side and a testis on the other (O/T), the oviduct and uterus are present only on the ovary side, and nothing derived from the Müllerian duct is present on the testis side. Here, we investigate the mechanism underlying the unilateral Müllerian duct regression and the mode of AMH signaling, by performing immunohistology, Western blotting, and organ culture analyses. The histological analysis revealed that during the start of the Müllerian duct regression, the duct in the O/T mice was clearly regressed on the AMH-positive testis side compared to the AMH-negative ovary side. The immunohistochemistry showed a diffuse immunoreaction of AMH in the interstitium surrounding the testis cord and boundary region between the testis and mesonephros, especially in the cranial portion. Western blotting revealed that the amount of AMH in the cranial half of the mesonephros was larger than that in the caudal half. AMH injected into the gonads in organ culture induced the regression of the Müllerian duct via the interstitium of the organ. These results suggest that AMH acts on the Müllerian duct in male mice by exuding into the interstitium surrounding the testis cord and infiltrating through the cranial region from the testis to the mesonephros.

KEY WORDS: AMH (anti-Müllerian hormone), Müllerian duct regression, secretion manner, sexual differentiation, true hermaphrodite

J. Vet. Med. Sci.
80(4): 557–567, 2018
doi: 10.1292/jvms.18-0023

Received: 14 January 2018
Accepted: 5 February 2018
Published online in J-STAGE: 9 March 2018

Ovaries in females (XX) and testes in males (XY) differ in morphology and function but share the same primordia. In early development, indifferent bipotential gonads arise in both sexes as a genital ridge and then differentiate into testes or ovaries. The fate of the gonads in mammals is determined by the XX/XY sex chromosome system, and particularly by the presence or absence of the *sex determining region of the Y chromosome* (*Sry*) [19].

For the realization of sexual multiplication, the formation of reproductive tracts as the migratory paths of germ cells is as important as the formation of gonads as the production sites of germ cells. Wolffian ducts [13, 25] and Müllerian ducts [8, 9, 26] are formed in both sexes during early development. They run in urogenital ridges as two pairs of ducts. In males, testicular secretions determine the fate of the ducts. Anti-Müllerian hormone (AMH) secreted from Sertoli cells induces the regression of the Müllerian ducts, and testosterone secreted from Leydig cells induces the development of Wolffian ducts into the epididymides, vasa deferens and seminal vesicles [4, 12, 14, 21]. On the other hand, because AMH and testosterone are absent from the developing female gonads, the Müllerian ducts develop into the oviducts, uterus and upper vagina, and the Wolffian ducts regress [14, 29].

AMH is a transforming growth factor-beta (TGF-β) superfamily member and is synthesized as a 140-kDa proprotein precursor (proAMH) homodimer that is incapable of binding to the AMH-specific receptor, anti-Müllerian hormone type 2 receptor

*Correspondence to: Hoshi, N.: nobhoshi@kobe-u.ac.jp

(AMHR2) [22]. ProAMH is cleaved by subtilisin/kexin proprotein convertases, yielding a 120-kDa N-terminal prodomain (AMH_N) and a 25-kDa C-terminal mature domain (AMH_C), and the latter is capable of binding AMHR2 [24]. AMHR2, a serine/threonine kinase, is expressed in the coelomic epithelial cells and subjacent mesenchymal cells lateral to the Müllerian duct of both male and female [3, 6, 28]. When AMH binds to AMHR2, the downstream signal is activated and the Müllerian duct regression is induced [23]. The Müllerian duct is regressed in the direction from the cranial to the caudal region [31] and the manner is presumably due to the cranial-to-caudal expression pattern of AMHR2 [1, 2].

The internal reproductive organs in our B6N-XY^{POS} mice, all of which are genetically male, can generally be classified into four phenotypes [32]: bilateral testes (T/T), accounting for approximately 36% of the mice; bilateral ovaries (O/O), accounting for 34%; true hermaphrodites (O/T), 20%; and bilateral ovotestes (OT/OT), 10% even though their sex chromosomal constitution is XY with *Sry*. Interestingly, in the O/T mice, the ovary side has female reproductive tract components such as the oviduct and uterus, whereas organs derived from Müllerian ducts have never been observed on the testis side. The unilateral regression of Müllerian ducts in true hermaphrodites is observed in not only the B6N-XY^{POS} mice but also other sex reversal mutant mice, such as *M33*-knockout mice [17] and *jumonji domain-containing protein 1a* (*Jmjd1a*)-knockout mice [20]. In addition, AMH effects have been shown to be ipsilateral, because unilateral orchiectomy in fetal rabbits resulted in Müllerian duct development only on the operated side [16]. The precise mechanism by which unilateral Müllerian duct regression is induced in the body remains unclear.

AMH is an important factor in the regression of the Müllerian ducts. When AMH acts on the Müllerian ducts in an endocrine manner through the circulatory system, the Müllerian ducts on both sides should regress. Therefore, although AMH is generally classified as a hormone, it appears not to act in an endocrine manner like hormones in the narrow sense. We hypothesized that AMH can act only on Müllerian ducts on one side in a secretory mode other than in the endocrine manner. Hence, we first examined the expression pattern for AMH and the degree of regression of the Müllerian duct in B6N-XY^{POS} mice during the fetal stage, and then investigated the mechanisms underlying Müllerian duct regression in normal male mice, focusing on AMH signaling.

MATERIALS AND METHODS

Animals

Male and female C57BL/6NCrSlc (B6N) mice embryos treated as normal phenotype and B6N-XY^{POS} mice embryos [32] were used, and all of their dams were maintained in 40.5 × 20.5 × 18.5-cm ventilated cages (Sealsafe Plus Mouse, Tecniplast, Buguggiate, Italy) under controlled temperature (23 ± 2°C), humidity (50 ± 10%) and ventilation (75 times/hr) on a 14-hr light/10-hr dark cycle at the Kobe University Life-Science Laboratory with *ad libitum* access to water and a pellet diet (DC-8, Clea Japan, Tokyo, Japan). This study was approved by the Institutional Animal Care and Use Committee (Permission #25-06-03) and carried out according to the Kobe University Animal Experimental Regulations.

Tissue preparation

The gonad-mesonephros complex was collected from 13.5 or 14.5 days post coitum (dpc) mice, for which 12:00 noon of the day of vaginal plug detection was designated as 0.5 dpc. The complex was fixed in 4% paraformaldehyde in 0.1 M phosphate buffer at 4°C for 2 hr or in Zamboni fixative at 4°C for 3 hr. The specimens were dehydrated with an ethanol series followed by xylene and then embedded in paraffin. Then, 4-μm-thick sections were cut by a sliding microtome (SM2000R, Leica Microsystems, Wetzlar, Germany), placed on slide glasses that had been precoated with 2% 3-aminopropyltriethoxysilan (Shin-Etsu Chemical, Tokyo, Japan), and rinsed in 1% Tween 20 before use.

Immunohistochemistry

After deparaffinization and hydration, the sections were heated at 121°C for 20 min in 10 mM sodium citrate buffer (pH 6.0) for antigen retrieval. The sections were allowed to return to room temperature, then immersed in absolute methanol for 30 min, followed by 0.5% H_2O_2 for 30 min to quench the endogenous peroxidase activity. Next, the sections were rinsed in 0.05% Tween 20-added 10 mM phosphate buffered saline (PBST) (pH 7.4), incubated with Blocking One Histo (Nacalai Tesque, Kyoto, Japan) at room temperature for 1 hr, and then reacted with primary antibodies in a humidified chamber at 4°C for 18 hr.

The primary antibodies used were as follows: anti-AMH goat polyclonal antibody (1:12,000 or 1:200; cat. #sc-6886, Santa Cruz Biotechnology, Santa Cruz, CA, U.S.A.), anti-SRY-box 9 (Sox9) rabbit polyclonal antibody (1:1,000; #sc-20095, Santa Cruz Biotechnology), and anti-forkhead box protein L2 (Foxl2) goat polyclonal antibody (1:800; #ab5096, Abcam, Cambridge, U.K.). These antibodies were used in serial sections. The sections were washed with PBST and incubated with horseradish peroxidase (HRP)-labeled polymer conjugated to secondary antibody (Dako EnVision®+ System-HRP Labeled Polymer Anti-Rabbit, Dako, Glostrup, Denmark) or alkaline phosphatase-labeled anti-goat IgG donkey antibody (1:100; #ab97112, Abcam) at room temperature for 1 hr.

The sections were washed with PBST, and the immunoreactivities of the primary antibodies were examined with 3,3-diaminobenzidine tetrahydrochloride solution (Dako EnVision®+ kit/HRP [DAB], Dako) or fuchsin solution (Dako Fuchsin+ Substrate-Chromogen System, Dako). Mayer's hematoxylin was used as a counterstain. The sections on which immunoreactivity was detected with the DAB system were placed in a graded series of ethanol, dehydrated with absolute ethanol, cleared in xylene and mounted in Eukitt® mounting medium (O. Kindler, Freiburg, Germany), and those detected with fuchsin were washed with distilled water and mounted in Aquatex® (Merck, Darmstadt, Germany).

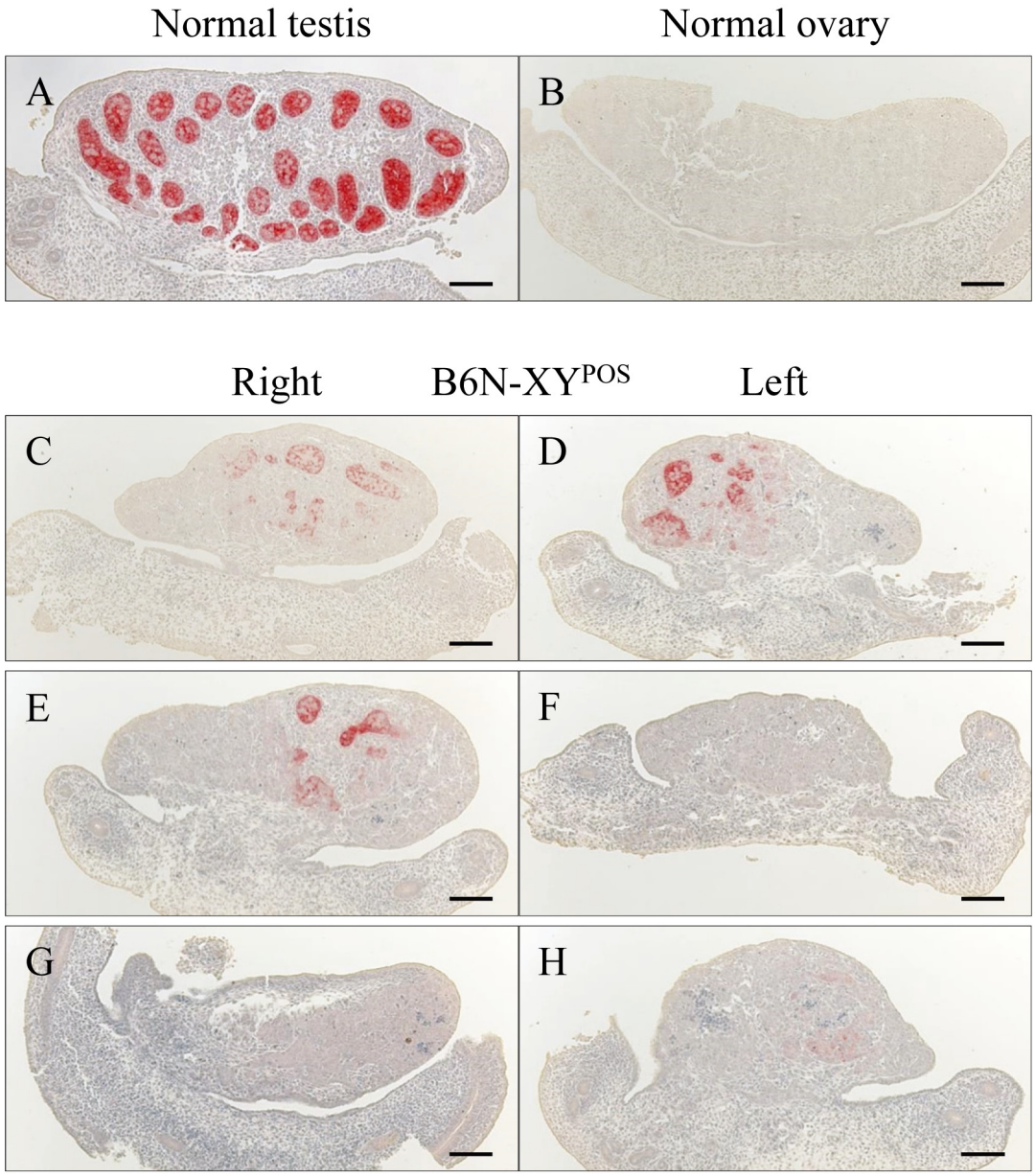

Fig. 1. Expression of AMH in sagittal sections of the gonad at 14.5 dpc in a normal male (A), normal female (B) and B6N-XY^{POS} mouse (C–H). Sertoli cells in the testis cord expressed AMH in the normal testis (A), and the normal ovary was negative for AMH expression (B). In the B6N-XY^{POS} mice, AMH was detected in a portion of both gonads (C and D), detected only in a portion of the right gonad (E and F) or rarely detected (G and H). Scale bars=100 μm.

Western blotting

The normal male mesonephros at 13.5 or 14.5 dpc was divided into the cranial and caudal region. The normal male gonad was used as a positive control and the normal female gonad-mesonephros complex was used as a negative control for AMH. The collected samples were snap-frozen in liquid nitrogen and stored at −80°C until use. Each sample was pooled in PCR tubes to adjust the protein amount: eight male bisectional mesonephroi, and four male gonads and three female gonad-mesonephros complexes. The proteins were separated by 15% sodium dodecyl sulfate-polyacrylamide gel electrophoresis (SDS-PAGE) at 200 V for 40 min and transferred to a 0.45-μm pore size Immobilon®-P Transfer Membranes (Merck) at 100 V for 1 hr, using a PowerPac™ High Current Power Supply (Bio-Rad Laboratories, Hercules, CA, U.S.A.). The membrane was cut between AMH (12.5 kDa) and glyceraldehyde-3-phosphate dehydrogenase (GAPDH) (37 kDa). We used a Precision Plus Protein™ WesternC™ Blotting Standards (#1610376, Bio-Rad Laboratories) as a guide for cutting.

After non-specific protein binding was blocked by incubation in Blocking One (Nacalai Tesque) at room temperature for 1 hr, each membrane was incubated at 4°C for 18 hr with anti-AMH goat polyclonal antibody (1:200; #sc-6886, Santa Cruz Biotechnology) or anti-GAPDH mouse monoclonal antibody (1:4,000; #016-25523, Wako, Tokyo, Japan) diluted with Blocking

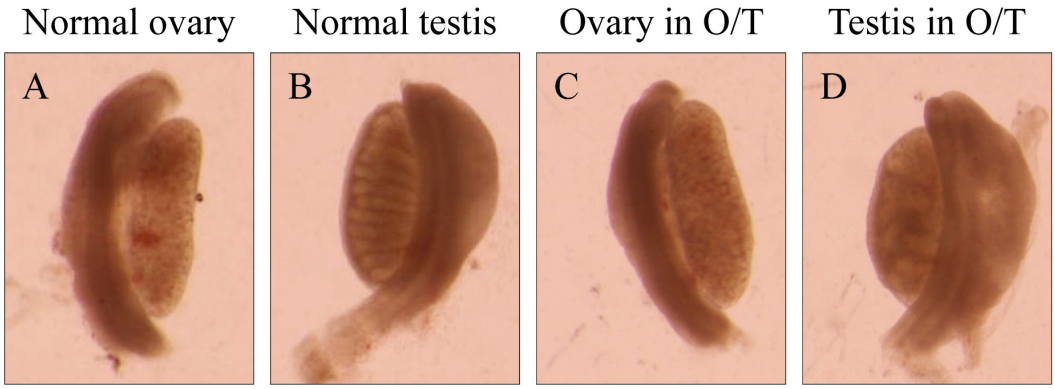

Fig. 2. The phenotypes of the gonads of a normal female (A), a normal male (B) and an O/T mouse (C and D) under a stereomicroscope at 14.5 dpc. The ovary (A) and testis (B) can be distinguished visually, because the testis is thickened and forms testis cords (B), and the ovary is not thickened and does not form testis cords (A). The ovary in the O/T mouse lacked testis cords (C) and was almost indistinguishable from the normal ovary (A). The testis in the same O/T mouse contained cord-like structures (D) and was similar in appearance to a normal testis (B).

One. We used the primary antibody recognizing the C-terminal region of AMH for the detection of AMH_C. After being washed with 0.1% Tween 20-added Tris-buffered saline (TBST) (25 mM Tris, 137 mM NaCl and 2.68 mM KCl; pH 7.4), each membrane was incubated with a HRP-labeled anti-goat IgG donkey antibody (1:20,000; #705-035-147, Jackson Immuno Research Laboratories, West Grove, PA, U.S.A.) or HRP-labeled anti-mouse IgG rat antibody (1:20,000; #415-035-166, Jackson Immuno Research Laboratories), respectively, at room temperature for 1 hr. The membranes were washed in TBST and reacted with a Chemi-Lumi One Super (Nacalai Tesque). The chemiluminescence signals were detected using a LuminoGraph I (ATTO, Tokyo, Japan). Quantification of the band intensity of AMH was performed using CS Analyzer (ATTO) and the relative amount of GAPDH was used as a loading control.

Organ culture

The normal male or female gonad-mesonephros complex at 13.5 dpc was incubated at 37°C with 5% CO_2 for 48 hr after the injection of 1 μl of recombinant human (rh)-AMH (100 μg/m*l*; #1737-MS, R&D Systems, Minneapolis, MN, U.S.A.) or normal saline (Otsuka Normal Saline, Otsuka Pharmaceutical Factory, Tokushima, Japan) into the gonad with mesonephros. The organ culture was performed on 1.5% agarose gel in 150 μl Dulbecco's Modified Eagle Medium (DMEM 4.5 g/*l* glucose with L-Gln and Sodium Pyruvate, Nacalai Tesque) supplemented with 10% KnockOut™ Serum Replacement (Gibco, Grand Island, NE, U.S.A.) instead of fetal bovine serum (FBS) to avoid effects of bovine AMH in the FBS, 100 IU/100 mg/m*l* penicillin/streptomycin, 3.48 mM L-glutamine and 1.87 mM pyruvate. Mebiol® Gel (Mebiol, Hiratsuka, Japan) was uniformly placed on the gonad to maintain the original form and the culture fluid was exchanged at 24 hr. In individual wells of a 24-well plate, one AMH-injected sample and one normal saline-injected sample were cultured in the same culture fluid. After the paraffin section of the tissues were prepared as described above, we used hematoxylin and eosin (HE) staining to evaluate the degree of regression of the Müllerian duct in each sample.

RESULTS

Histology of B6N-XY^{POS} mice

We detected AMH in the Sertoli cells forming testis cords in the normal male gonads at 14.5 dpc (which is when the regression of the mouse Müllerian ducts begins) (Fig. 1A), whereas there were no AMH-positive cells in the normal female gonads at that time (Fig. 1B). In the B6N-XY^{POS} mice, the degree of AMH immunoreaction varied among gonads even in the same animal. We observed that AMH-positive cells were unevenly located in both gonads (Fig. 1C and 1D), one gonad (Fig. 1E and 1F) or neither of the gonads (Fig. 1G and 1H). The number of AMH-positive cells and the intensity of the immunoreaction were clearly less in all of the B6N-XY^{POS} mice compared to the normal males (Fig. 1).

We examined the AMH expression and the degree of Müllerian duct regression in three O/T mice by separating the 14.5 dpc samples into the cranial, middle and caudal regions. At that time point, the gonads can already be discriminated as an ovary (Fig. 2A) or a testis (Fig. 2B) under a stereomicroscope. One gonad from an O/T mouse showed an ovary-like structure in which the testis cord was not observed clearly (Fig. 2C), and the other gonad in the same mouse was thickened like a testis and had ambiguous cord-like structures resembling testis cords (Fig. 2D).

The transverse sections revealed that the ovaries in the O/T mice expressed Foxl2, a marker of granulosa cells, throughout the whole length (Fig. 3A), and Sox9, a marker of Sertoli cells, was detected in serial sections, especially in the middle portion, where the Foxl2 expression was weak (Fig. 3B). No AMH-positive cells were detected in the Foxl2-dominant ovary in the O/T mice, even in the region where Sox9 was detected (Fig. 3C). In contrast, the testes in the O/T mice showed slight to strong Sox9

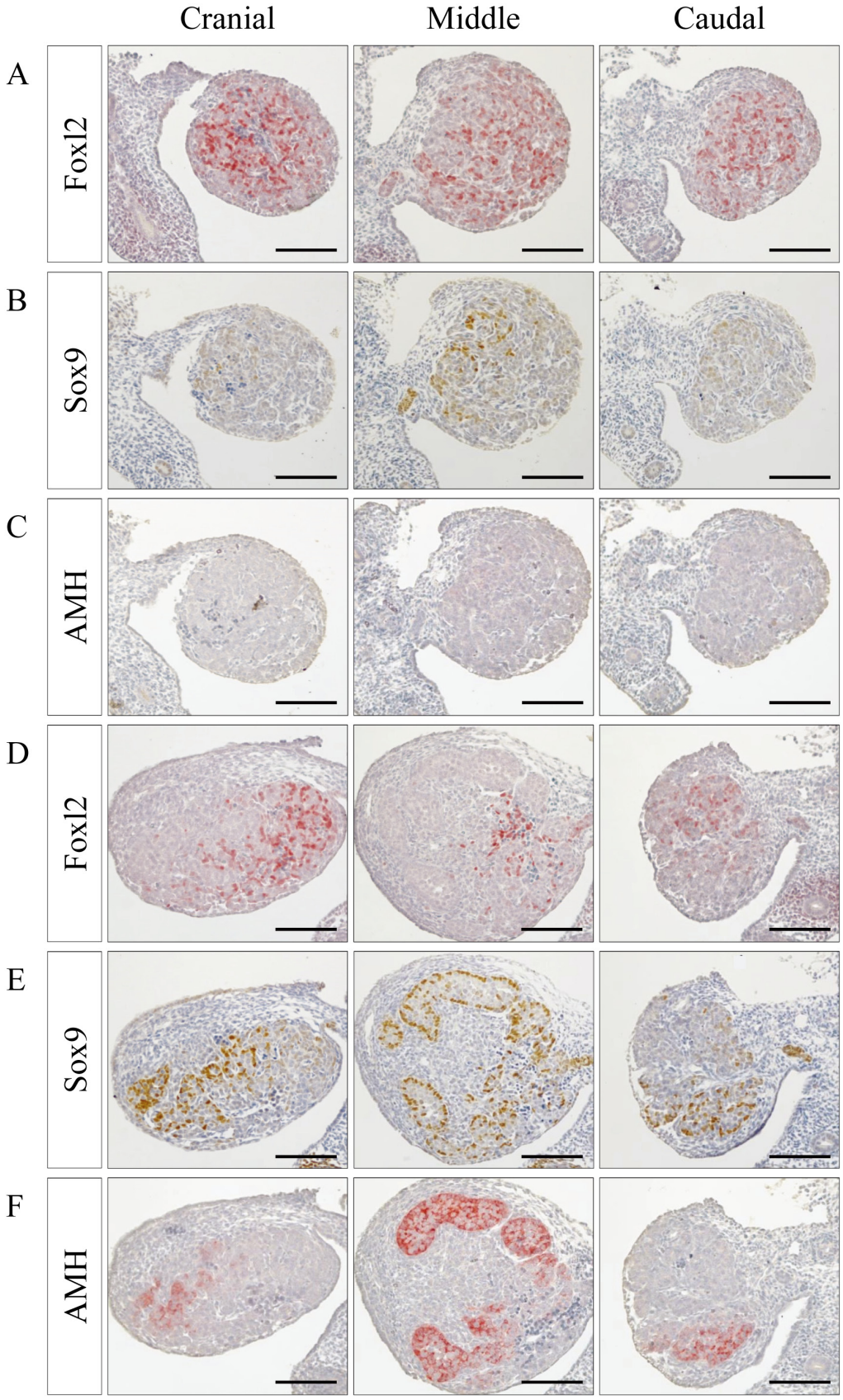

Fig. 3. The transverse sections of the cranial, middle and caudal portions of the ovary (A–C) and testis (D–F) of an O/T mouse at 14.5 dpc. Immunoreactivity of Foxl2, a marker of granulosa cells (A and D), Sox9, a marker of Sertoli cells (B and E) and AMH (C and F) in the gonads of the O/T mouse are shown, with the appearance shown in Fig. 2C and 2D. In the ovary from the O/T mouse, Foxl2 was expressed along the whole length (A) and AMH was negative (C). In the testis from the O/T mouse, Sox9 was detected through the entire length, and the testis cords were clearly visualized especially in the middle portion (E), whereas AMH was detected in some of the Sox9-positive regions (F). Scale bars=100 μm.

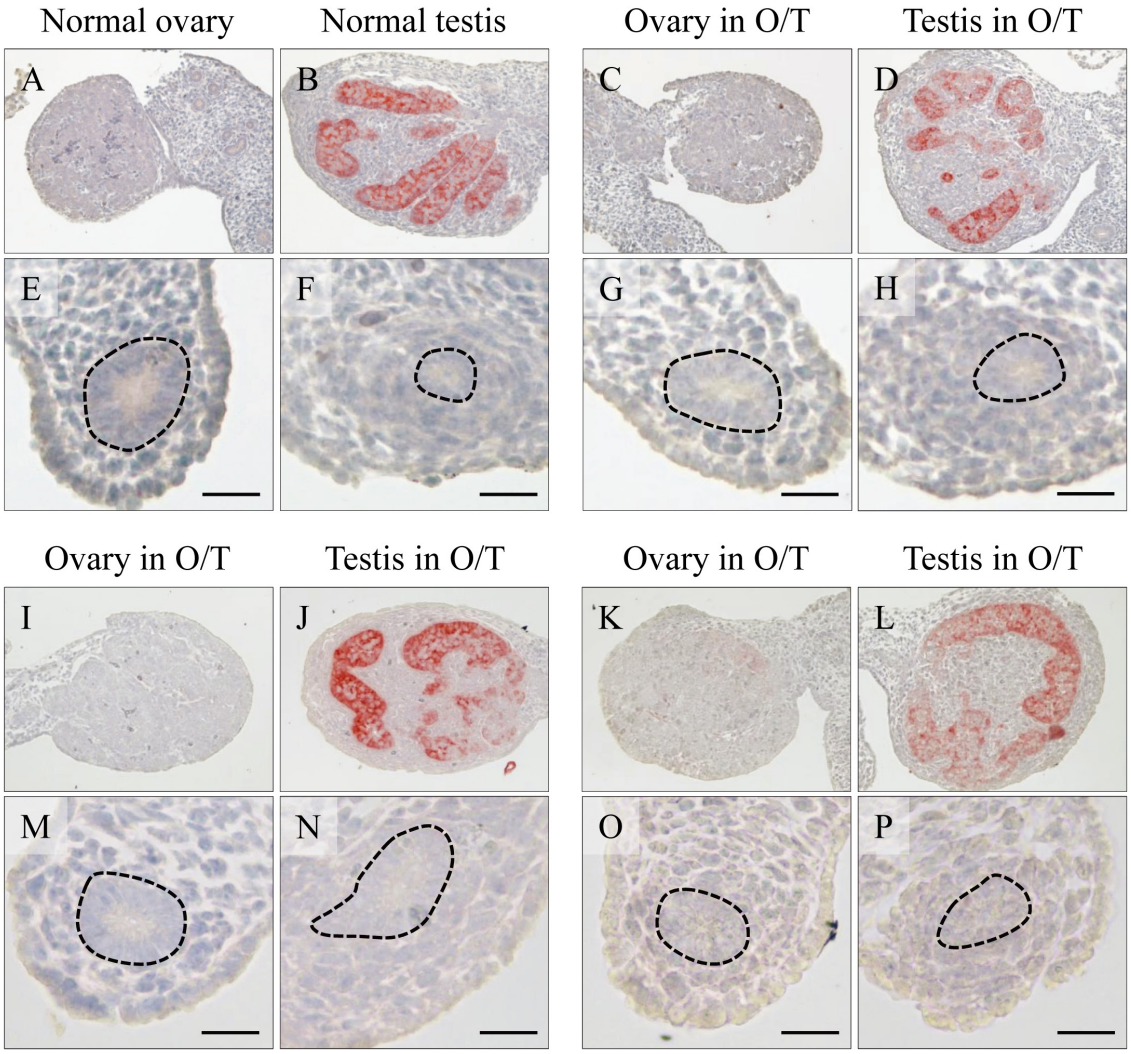

Fig. 4. The expression of AMH at 14.5 dpc in the normal ovary (A), normal testis (B), ovary in O/T mice (C, I and K) and testis in O/T mice (D, J and L), and the respective Müllerian ducts in transverse sections (E–H and M–P). In the normal males, the diameter of the Müllerian ducts was small and the mesenchymal cells surrounding the Müllerian ducts were condensed and formed a swirl pattern (F), whereas those in the normal females did not exhibit these features (E). The mesenchymal cells surrounding Müllerian ducts of the ovary (G, M and O) and testis (H, N and P) in the O/T mice were similar to those of the normal phenotype (E and F), respectively. In addition, the ratio of the Müllerian duct diameter to the width of the mesonephros on the testis side (H, N and P) was smaller than that on the ovary side (G, M and O). The dashed line indicates the basal line of the Müllerian duct epithelium. Scale bars=20 μm.

expression over the entire length, and some testis cords comprised of Sox9-positive cells were observed, especially in the middle portion (Fig. 3E), although some Foxl2 expression was also detected in Sox9-negative regions (Fig. 3D). AMH-positive cells were observed in some portions of the Sox9-positive site along the gonad, but the strength of the positivity was weak and the numbers of these cells were small, especially at the two poles (Fig. 3F).

The transverse sections of the normal males showed that the mesenchymal cells were closely gathered in a vortical manner around the epithelium of the Müllerian duct, and the Müllerian duct diameter was small (Fig. 4F); these findings were not observed in the normal females (Fig. 4E). The state of the mesenchymal cells of the ovary side in the O/T mice (Fig. 4G, 4M and 4O) was similar to that of the normal females (Fig. 4E). On the other hand, the mesenchymal cells of the testis side in the O/T mice (Fig. 4H, 4N and 4P) were in the process of being condensed and forming a swirl pattern as in the normal testes (Fig. 4F). In addition, on the testis side in the O/T mice, the diameter of the Müllerian duct relative to the width of the mesonephros (Fig. 4H, 4N and 4P) was smaller than that on the ovary side (Fig. 4G, 4M and 4O), although the diameter (Fig. 4H, 4N and 4P) was not as small as that on the normal males (Fig. 4F).

Detection of AMH secretion in the interstitium of the normal testes

We next attempted to detect small amounts of AMH secreted into the interstitium of the testes by using the anti-AMH antibody at a higher concentration. Unsurprisingly, as shown in the sagittal sections, AMH was expressed in Sertoli cells, and the diffusing

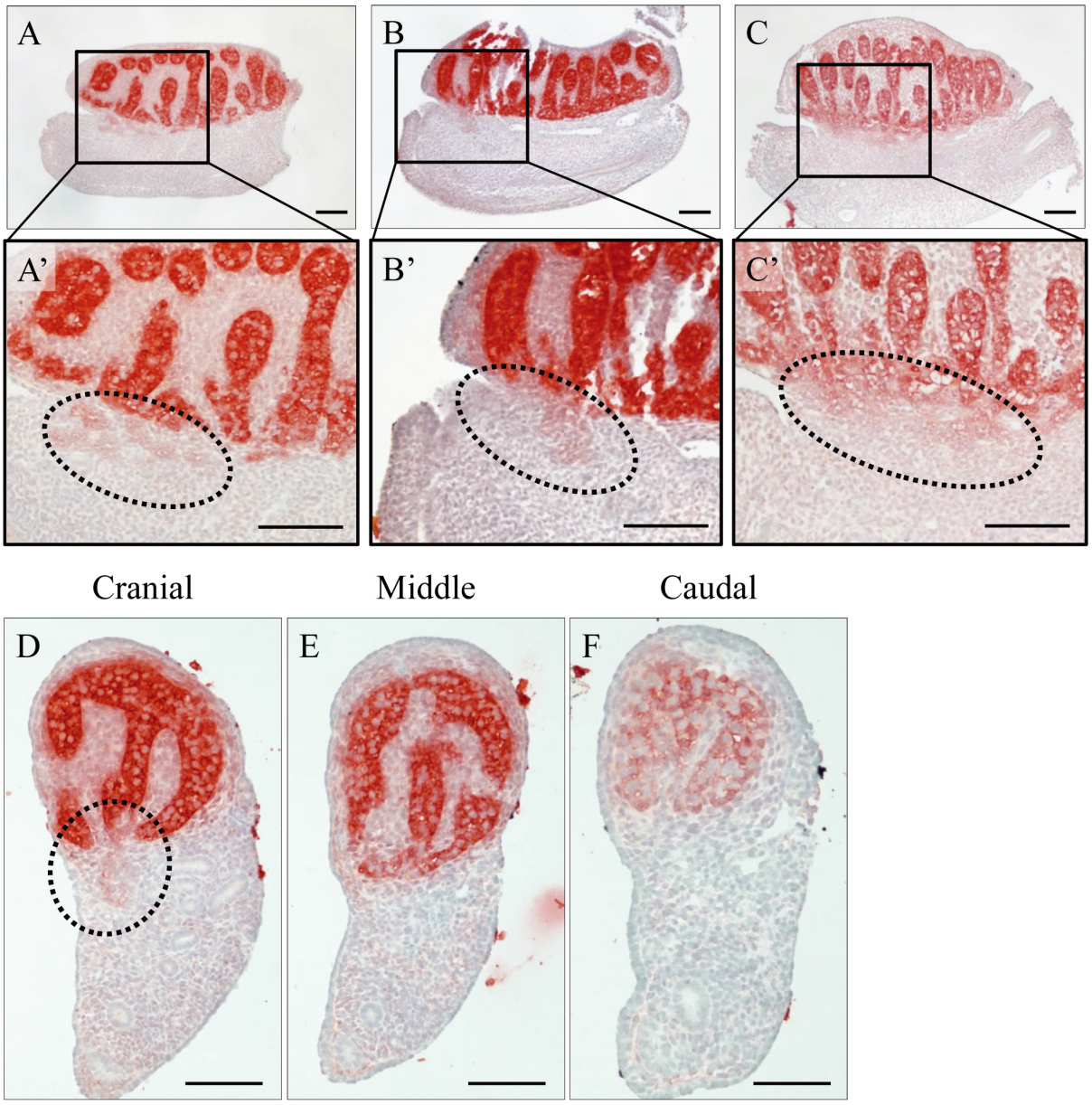

Fig. 5. Immunoreaction of AMH secretion in a sagittal section of a normal testis at 13.5 (A and B) or 14.5 dpc (C) and transverse sections of a normal testis at 13.5 dpc (D–F). AMH was strongly detected in Sertoli cells and weakly detected in the interstitium of the testis (A–F). In addition, a diffused immunoreaction was observed in the boundary region between the testis and mesonephros in one part of the cranial region (dashed line in A'–C' and D). In the sagittal sections, the left side of each panel is the cranial region and the right side is the caudal region. Scale bars=100 μm.

immunoreaction was detected in the interstitium around the testis cords at 13.5 and 14.5 dpc (Fig. 5A–C). In addition, in one part of the cranial region, a weak immunoreaction toward the mesonephros was observed (Fig. 5A'–C'). The same pattern was also observed in the transverse sections divided into three parts, *i.e.*, the cranial (Fig. 5D), middle (Fig. 5E) and caudal (Fig. 5F) regions. In only the cranial region, a weak positive reaction toward the mesonephros was observed around the boundary region between the testis and mesonephros (Fig. 5D).

AMH concentrations in the cranial/caudal mesonephros of the normal mice

Based on the above findings, we expected the concentration of AMH to be higher in the cranial region than in the caudal region of the normal male mesonephros. We thus performed Western blotting to measure the levels of secreted C-terminal AMH in the male mesonephroi, male gonads (as a positive control for AMH) and female gonad-mesonephros complexes (as a negative control for AMH). The band corresponding to C-terminal AMH was observed at 12.5 kDa (Fig. 6A) in the male gonads and the male mesonephroi, but not in the female gonad-mesonephros complexes. The density of each band was measured and the data were

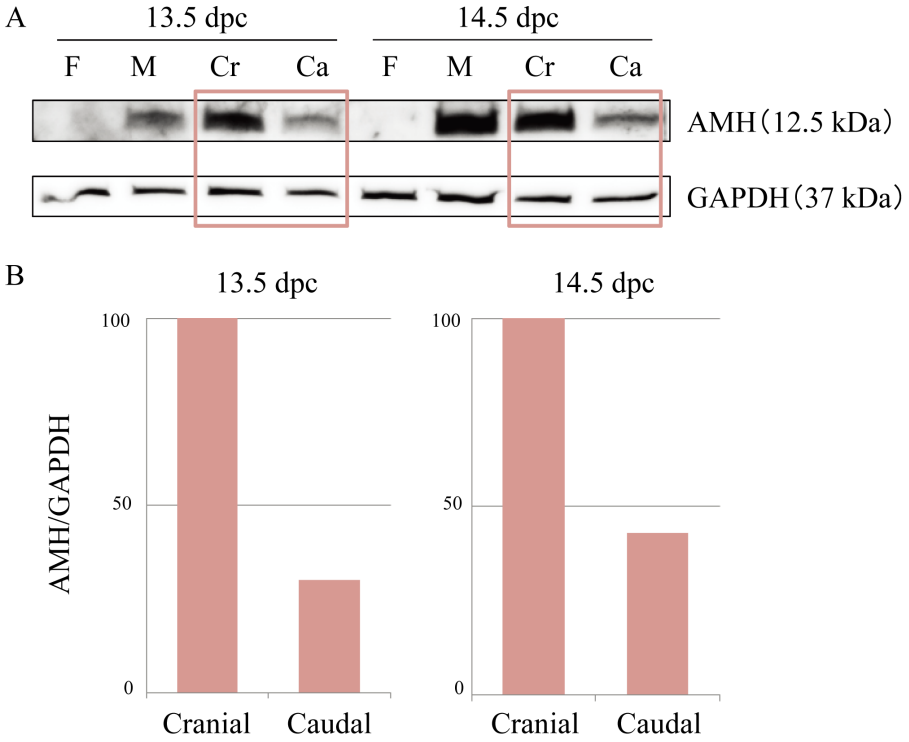

Fig. 6. A: AMH expression in the cranial/caudal mesonephroi at 13.5 and 14.5 dpc in normal males by Western blotting. Normal female gonad-mesonephros complexes were used as a negative control for AMH, and normal male gonads were used as a positive control for AMH. AMH bands (12.5 kDa) were detected in male gonads and cranial/caudal mesonephros, and GAPDH bands (37 kDa) were visualized in all samples. B: The amounts of AMH in the cranial and caudal mesonephros. The band intensity of AMH was quantified by using the value of the GAPDH bands. When the amount of AMH in the cranial mesonephros is set at 100, the amount in the caudal mesonephros is less than half as large at both 13.5 and 14.5 dpc. F: female gonad-mesonephros complexes; M: male gonads; Cr: cranial half of the male mesonephroi; Ca: caudal half of the male mesonephroi.

normalized using the value of the GAPDH band at 37 kDa. The level of AMH protein in the cranial mesonephroi was higher than that in the caudal mesonephroi at both 13.5 and 14.5 dpc. The amount of AMH in the caudal mesonephroi was approximately one-third of that in the cranial mesonephroi at 13.5 dpc and less than half that in the cranial mesonephroi at 14.5 dpc (Fig. 6B).

Dynamics of AMH in the organ culture

To investigate the dynamics of AMH in an organ culture of normal male and female gonad-mesonephros complex, we injected rh-AMH or normal saline into gonads with mesonephroi. After 48 hr of incubation the degree of regression of the Müllerian duct in each sample was evaluated. These two types of gonad-mesonephros complexes were cultured in the same well to eliminate the influence of AMH that may have leaked into the medium. The degree of regression of the Müllerian ducts in the AMH-injected samples (Fig. 7B, 7D, 7F and 7H) was clearly larger than that in the normal saline-injected samples (Fig. 7A, 7C, 7E and 7G) at the same cranial and caudal positions.

DISCUSSION

We investigated the mode of AMH signaling using B6N-XY^{POS} mice and normal mice. The immunohistological analysis revealed that the level of AMH produced and secreted in the B6N-XY^{POS} mice was less than that in the normal males, and AMH-positive cells were detected mainly in the middle region of the gonads of the B6N-XY^{POS} mice. The existence of AMH^{-}/Sox9^{+} incompletely differentiated Sertoli cells was also confirmed.

Sry expression begins in the middle region of the gonad, then extends to both poles [5]. Normal testis development requires that sufficient *Sry* expression is maintained for a critical time window of at least 6 hr at approximately 11.0–11.25 dpc [11]. In our study of the expression of testicular genes in B6N-XY^{POS} mice, although *Sry* was expressed in the same manner as in normal males, *Sry* and its downstream gene, *Sox9*, occurred at 2–3 tail somites later in the B6N-XY^{POS} mice compared to normal males [32]. In the B6N-XY^{POS} mice examined in the present study, the Sry expression appeared to be insufficient at both poles of the gonad, and this

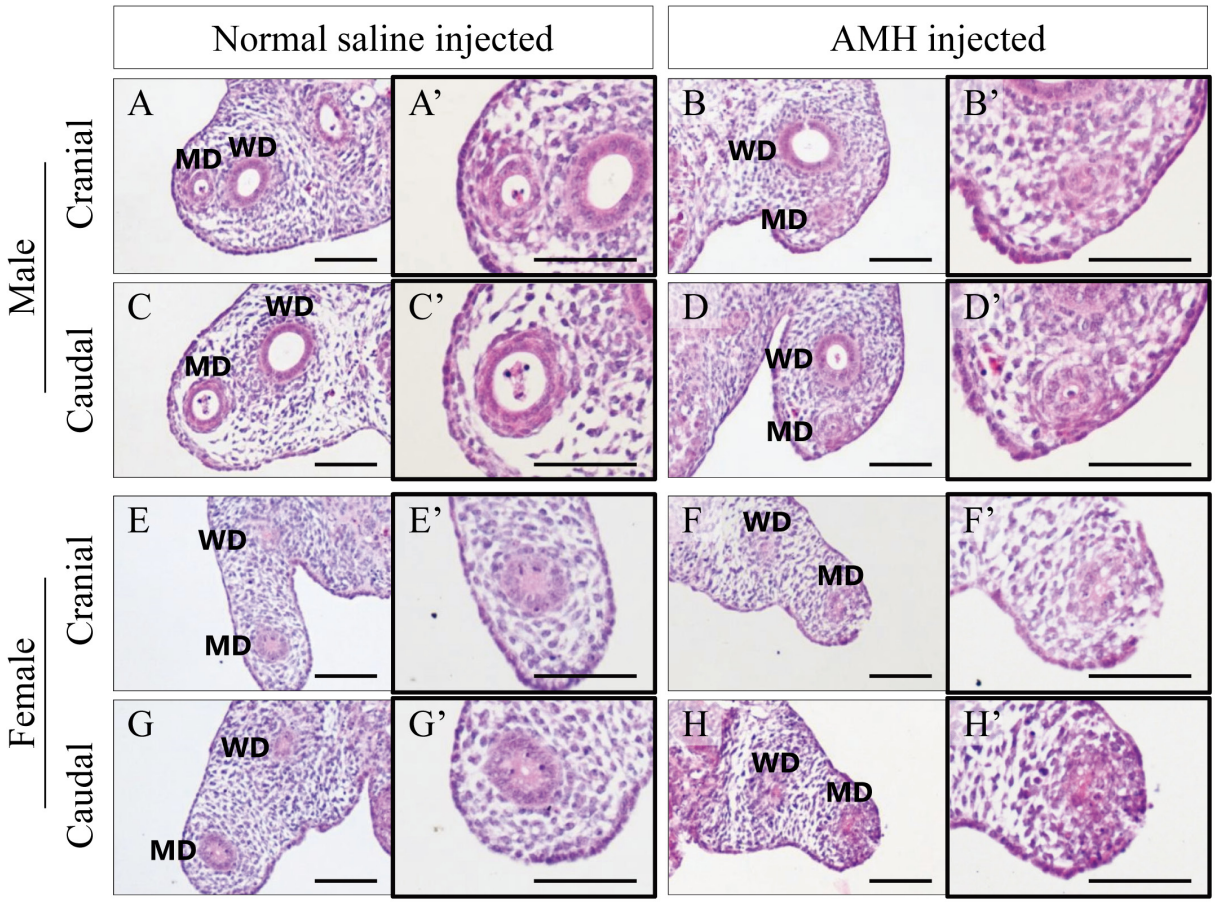

Fig. 7. HE staining for the urogenital ridges of normal male and normal female in an organ culture (A–H) and magnified images focusing on the Müllerian ducts (A'–H'). The Müllerian ducts with AMH (B, D, F and H) are clearly more regressed than those with normal saline (A, C, E and G) at the same height of the mesonephros, respectively. Scale bars=100 μm.

lack of expression might have induced the incompletely differentiated Sertoli cells, which expressed Sox9 but could not synthesize AMH, especially at the poles. Even if the gonad appears to develop into a testis with Sox9-positive cells, the cells might not synthesize AMH in these specific situations.

These results suggest that a critical time window of Sry action may exist for the differentiation of normally functioning Sertoli cells that synthesize AMH. It would thus be useful to reconsider the critical window of Sry more strictly compared to the study cited above [11] in a certain genetic backgrounds. It should be noted that the use of Sox9 as a marker of Sertoli cells may include the risk that some of the Sox9-positive cells will be non-functional Sertoli cells with no AMH expression.

When the Müllerian duct regresses, the mesenchymal cells surrounding the Müllerian duct condense and form a swirl pattern [7, 26, 33], and the diameter of the Müllerian duct becomes small. In the present study, the degree of regression of the Müllerian ducts was smaller in the B6N-XY^{POS} mice (with less AMH secretion) compared to the normal males, suggesting that the degree of Müllerian duct regression was dependent on the amount of AMH secreted. More importantly, the state of mesenchymal cells and the diameter of the Müllerian ducts in the O/T mice suggested that the Müllerian duct of the AMH-negative side hardly regressed, whereas the duct of the AMH-positive side showed steadily progressing regression. At the time point when the Müllerian ducts began to regress in the normal males, significant regression of the ducts was observed only on the side of the testis in the O/T mice that secreted AMH, as has been shown in adult O/T mice [32].

To account for this phenomenon, we first performed immunohistochemistry using the primary antibody at a high concentration on the normal testis. A weak AMH-positive reaction was detected in the testicular interstitium and the cranial boundary region between the testis and mesonephros. This may indicate that AMH, following its secretion by Sertoli cells, flows into the interstitium surrounding the testis cord and then infiltrates the Müllerian duct in the mesonephros from the cranial region of the testis.

If this hypothesis is correct, the amount of AMH in the mesonephros would be expected to be larger in the cranial part than in the caudal part. The cleavage of proAMH occurs in the gonads, and the ratio of both proAMH and $AMH_{N,C}$ are not altered after the release from the gonads [27]. Therefore, in the mesonephros, 12.5-kDa AMH_C will be detected as functional AMH that is able to bind to AMHR2. As we expected, the amount of AMH detected in the cranial mesonephroi by Western blotting was larger than that detected in the caudal mesonephroi, supporting the hypothesis that AMH infiltrates from the testis to the mesonephros, especially at

the cranial region, and acts on the Müllerian ducts.

In the organ culture, an increase in the degree of Müllerian duct regression was observed only in the AMH-injected samples, even though we eliminated the influence of AMH flow into the medium from the gonads. We thus speculate that AMH injected into the gonads infiltrated the Müllerian ducts and triggered their regression.

For the experiments of the Müllerian duct regression, organ culture analysis of urogenital ridge adding rh-AMH to the culture fluid is commonly used methods [31, 34, 35]. In the present study, we injected rh-AMH directly into the gonads instead of adding it to the culture medium. That was closer to *in vivo* situation and might be able to reproduce more accurate dynamics of AMH.

The rete testis, which gathers seminal fluid from the seminiferous tubules, is formed at the cranial region of the testis and connects the efferent ductules in the epididymis. The surface of the testis is covered with the tunica albuginea, and the efferent ductules link the rete testis to the epididymis, piercing the tunica albuginea [18]. At 13.5 and 14.5 dpc, the tunica albuginea separating the testis and mesonephros may be absent in the cranial region where the rete testis is formed in later development. Thus, the lack of the tunica albuginea may be a reason why AMH infiltrates from the testis into the Müllerian duct, especially through the cranial region.

The Müllerian duct regression is hypothesized to occur in a cranial-to-caudal manner corresponding to the expression of AMHR2. AMHR2-expressing cells are initially present in the mesonephric epithelium and mesenchyme on the anti-mesometrial side of both males and females equally. Under the influence of AMH, the cells proliferate and migrate into the mesenchyme surrounding the Müllerian duct [10, 30, 35]. The flow of secreted AMH suggested in the present study may therefore explain why the regression starts at the cranial part of the Müllerian duct. In other words, the pattern of secretion shown in this study could be applicable to normal male mice *in vivo*. It is necessary to verify the cause of the regression of the caudal region of Müllerian ducts by determining whether (i) the infiltration from the cranial testis reaches the caudal side or (ii) the signal entering the cranial region propagates to the caudal region.

Many studies of AMH and Müllerian duct regression have been conducted since the first report that testicular factor, distinct from testosterone, is responsible for Müllerian duct regression during male sex differentiation [15]. However, the detailed mechanisms by which AMH exerts its ipsilateral effects have been unclear. Our present findings elucidate the precise mechanisms by which AMH flow induces the regression of Müllerian ducts in the developing embryo. AMH secreted by the testis may induce an ipsilateral regression of the Müllerian duct by its secretion into the interstitium surrounding the testis cord and its subsequent infiltration into the cranial region between the testis and mesonephros.

ACKNOWLEDGMENTS. This work was supported by Grants-in-Aid for Scientific Research (nos. 24590401 and 16K08072 to N. Hoshi) and (nos. 26460410 and 17K08686 to T. Yokoyama) from the Ministry of Education, Culture, Sports, Science and Technology of Japan.

REFERENCES

1. Allard, S., Adin, P., Gouédard, L., di Clemente, N., Josso, N., Orgebin-Crist, M. C., Picard, J. Y. and Xavier, F. 2000. Molecular mechanisms of hormone-mediated Müllerian duct regression: involvement of β-catenin. *Development* **127**: 3349–3360. [Medline]
2. Arango, N. A., Kobayashi, A., Wang, Y., Jamin, S. P., Lee, H. H., Orvis, G. D. and Behringer, R. R. 2008. A mesenchymal perspective of Müllerian duct differentiation and regression in *Amhr2-lacZ* mice. *Mol. Reprod. Dev.* **75**: 1154–1162. [Medline] [CrossRef]
3. Baarends, W. M., van Helmond, M. J. L., Post, M., van der Schoot, P. J. C. M., Hoogerbrugge, J. W., de Winter, J. P., Uilenbroek, J. T. J., Karels, B., Wilming, L. G., Meijers, J. H. C., Themmen, A. P. N. and Grootegoed, J. A. 1994. A novel member of the transmembrane serine/threonine kinase receptor family is specifically expressed in the gonads and in mesenchymal cells adjacent to the müllerian duct. *Development* **120**: 189–197. [Medline]
4. Behringer, R. R., Finegold, M. J. and Cate, R. L. 1994. Müllerian-inhibiting substance function during mammalian sexual development. *Cell* **79**: 415–425. [Medline] [CrossRef]
5. Bullejos, M. and Koopman, P. 2001. Spatially dynamic expression of *Sry* in mouse genital ridges. *Dev. Dyn.* **221**: 201–205. [Medline] [CrossRef]
6. di Clemente, N., Wilson, C., Faure, E., Boussin, L., Carmillo, P., Tizard, R., Picard, J. Y., Vigier, B., Josso, N. and Cate, R. 1994. Cloning, expression, and alternative splicing of the receptor for anti-Müllerian hormone. *Mol. Endocrinol.* **8**: 1006–1020. [Medline]
7. Dyche, W. J. 1979. A comparative study of the differentiation and involution of the Müllerian duct and Wolffian duct in the male and female fetal mouse. *J. Morphol.* **162**: 175–209. [Medline] [CrossRef]
8. Fujino, A., Arango, N. A., Zhan, Y., Manganaro, T. F., Li, X., MacLaughlin, D. T. and Donahoe, P. K. 2009. Cell migration and activated PI3K/AKT-directed elongation in the developing rat Müllerian duct. *Dev. Biol.* **325**: 351–362. [Medline] [CrossRef]
9. Guioli, S., Sekido, R. and Lovell-Badge, R. 2007. The origin of the Mullerian duct in chick and mouse. *Dev. Biol.* **302**: 389–398. [Medline] [CrossRef]
10. Hayashi, A., Donahoe, P. K., Budzik, G. P. and Trelstad, R. L. 1982. Periductal and matrix glycosaminoglycans in rat Mullerian duct development and regression. *Dev. Biol.* **92**: 16–26. [Medline] [CrossRef]
11. Hiramatsu, R., Matoba, S., Kanai-Azuma, M., Tsunekawa, N., Katoh-Fukui, Y., Kurohmaru, M., Morohashi, K., Wilhelm, D., Koopman, P. and Kanai, Y. 2009. A critical time window of *Sry* action in gonadal sex determination in mice. *Development* **136**: 129–138. [Medline] [CrossRef]
12. Ingraham, H. A., Hirokawa, Y., Roberts, L. M., Mellon, S. H., McGee, E., Nachtigal, M. W. and Visser, J. A. 2000. Autocrine and paracrine Müllerian inhibiting substance hormone signaling in reproduction. *Recent Prog. Horm. Res.* **55**: 53–67, discussion 67–68. [Medline]
13. Jacob, M., Christ, B., Jacob, H. J. and Poelmann, R. E. 1991. The role of fibronectin and laminin in development and migration of the avian Wolffian duct with reference to somitogenesis. *Anat. Embryol. (Berl.)* **183**: 385–395. [Medline] [CrossRef]
14. Josso, N., Lamarre, I., Picard, J. Y., Berta, P., Davies, N., Morichon, N., Peschanski, M. and Jeny, R. 1993. Anti-Müllerian hormone in early human development. *Early Hum. Dev.* **33**: 91–99. [Medline] [CrossRef]

15. Jost, A. 1947. Recherches sur la différenciation sexuelle de l'embryon de lapin. *Arch. Anat. Microsc. Morphol. Exp.* **36**: 271–315.
16. Jost, A. 1953. Problems of fetal endocrinology: The gonadal and hypophyseal hormones. *Recent Prog. Horm. Res.* **8**: 379–418.
17. Katoh-Fukui, Y., Tsuchiya, R., Shiroishi, T., Nakahara, Y., Hashimoto, N., Noguchi, K. and Higashinakagawa, T. 1998. Male-to-female sex reversal in *M33* mutant mice. *Nature* **393**: 688–692. [Medline] [CrossRef]
18. Kierszenbaum, A. L. and Tres, L. L. 2012. Sperm transport and maturation. pp. 617–631. *In*: Histology and Cell Biology. 3rd ed., Elsevier, Philadelphia.
19. Koopman, P., Gubbay, J., Vivian, N., Goodfellow, P. and Lovell-Badge, R. 1991. Male development of chromosomally female mice transgenic for *Sry*. *Nature* **351**: 117–121. [Medline] [CrossRef]
20. Kuroki, S., Matoba, S., Akiyoshi, M., Matsumura, Y., Miyachi, H., Mise, N., Abe, K., Ogura, A., Wilhelm, D., Koopman, P., Nozaki, M., Kanai, Y., Shinkai, Y. and Tachibana, M. 2013. Epigenetic regulation of mouse sex determination by the histone demethylase Jmjd1a. *Science* **341**: 1106–1109. [Medline] [CrossRef]
21. Lee, M. M. and Donahoe, P. K. 1993. Mullerian inhibiting substance: a gonadal hormone with multiple functions. *Endocr. Rev.* **14**: 152–164. [Medline]
22. MacLaughlin, D. T., Hudson, P. L., Graciano, A. L., Kenneally, M. K., Ragin, R. C., Manganaro, T. F. and Donahoe, P. K. 1992. Mullerian duct regression and antiproliferative bioactivities of Mullerian inhibiting substance reside in its carboxy-terminal domain. *Endocrinology* **131**: 291–296. [Medline] [CrossRef]
23. Mishina, Y., Whitworth, D. J., Racine, C. and Behringer, R. R. 1999. High specificity of Müllerian-inhibiting substance signaling *in vivo*. *Endocrinology* **140**: 2084–2088. [Medline] [CrossRef]
24. Nachtigal, M. W. and Ingraham, H. A. 1996. Bioactivation of Müllerian inhibiting substance during gonadal development by a kex2/subtilisin-like endoprotease. *Proc. Natl. Acad. Sci. U.S.A.* **93**: 7711–7716. [Medline] [CrossRef]
25. Obara-Ishihara, T., Kuhlman, J., Niswander, L. and Herzlinger, D. 1999. The surface ectoderm is essential for nephric duct formation in intermediate mesoderm. *Development* **126**: 1103–1108. [Medline]
26. Orvis, G. D. and Behringer, R. R. 2007. Cellular mechanisms of Müllerian duct formation in the mouse. *Dev. Biol.* **306**: 493–504. [Medline] [CrossRef]
27. Pankhurst, M. W., Leathart, B. L. A., Batchelor, N. J. and McLennan, I. S. 2016. The anti-Müllerian hormone precursor (proAMH) is not converted to the receptor-competent form ($AMH_{N,C}$) in the circulating blood of mice. *Endocrinology* **157**: 1622–1629. [Medline] [CrossRef]
28. Teixeira, J., He, W. W., Shah, P. C., Morikawa, N., Lee, M. M., Catlin, E. A., Hudson, P. L., Wing, J., Maclaughlin, D. T. and Donahoe, P. K. 1996. Developmental expression of a candidate Müllerian inhibiting substance type II receptor. *Endocrinology* **137**: 160–165. [Medline] [CrossRef]
29. Teixeira, J., Maheswaran, S. and Donahoe, P. K. 2001. Müllerian inhibiting substance: an instructive developmental hormone with diagnostic and possible therapeutic applications. *Endocr. Rev.* **22**: 657–674. [Medline]
30. Trelstad, R. L., Hayashi, A., Hayashi, K. and Donahoe, P. K. 1982. The epithelial-mesenchymal interface of the male rate Mullerian duct: loss of basement membrane integrity and ductal regression. *Dev. Biol.* **92**: 27–40. [Medline] [CrossRef]
31. Tsuji, M., Shima, H., Yonemura, C. Y., Brody, J., Donahoe, P. K. and Cunha, G. R. 1992. Effect of human recombinant Mullerian inhibiting substance on isolated epithelial and mesenchymal cells during Mullerian duct regression in the rat. *Endocrinology* **131**: 1481–1488. [Medline] [CrossRef]
32. Umemura, Y., Miyamoto, R., Hashimoto, R., Kinoshita, K., Omotehara, T., Nagahara, D., Hirano, T., Kubota, N., Minami, K., Yanai, S., Masuda, N., Yuasa, H., Mantani, Y., Matsuo, E., Yokoyama, T., Kitagawa, H. and Hoshi, N. 2016. Ontogenic and morphological study of gonadal formation in genetically-modified sex reversal XY^{POS} mice. *J. Vet. Med. Sci.* **77**: 1587–1598. [Medline] [CrossRef]
33. Wartenberg, H. 1985. Morphological studies on the role of the periductal stroma in the regression of the human male Müllerian duct. *Anat. Embryol. (Berl.)* **171**: 311–323. [Medline] [CrossRef]
34. Wilson, C. A., di Clemente, N., Ehrenfels, C., Pepinsky, R. B., Josso, N., Vigier, B. and Cate, R. L. 1993. Mullerian inhibiting substance requires its N-terminal domain for maintenance of biological activity, a novel finding within the transforming growth factor-β superfamily. *Mol. Endocrinol.* **7**: 247–257. [Medline]
35. Zhan, Y., Fujino, A., MacLaughlin, D. T., Manganaro, T. F., Szotek, P. P., Arango, N. A., Teixeira, J. and Donahoe, P. K. 2006. Müllerian inhibiting substance regulates its receptor/SMAD signaling and causes mesenchymal transition of the coelomic epithelial cells early in Müllerian duct regression. *Development* **133**: 2359–2369. [Medline] [CrossRef]